Annals of Glaciology 29 1999

Monte Carlo inverse modelling of the Law Dome (Antarctica) temperature profile

Dorthe Dahl-Jensen,[1] Vin I. Morgan,[2] Alan Elcheikh[2]
[1]*The Niels Bohr Institute for Astronomy, Physics and Geophysics, University of Copenhagen, DK-2100 Copenhagen, Denmark*
[2]*Antarctic CRC and Australian Antarctic Division, Box 252-80, Hobart, Tasmania 7001, Australia*

ABSTRACT. The temperature profile in the 1200 m deep Dome Summit South (DSS) borehole near the summit of Law Dome, Antarctica, was measured in 1996, 3 years after the termination of the deep drilling.

The temperature profile contains information on past surface temperature over the last 4 ka. This temperature history is determined by the use of a Monte Carlo inverse method in which no constraints are placed on the unknown temperature history and no solution is assumed to be unique. The temperature history is obtained from a selection of equally well-fitting solutions by a statistical treatment.

The results show that solutions covering the last 4 ka have a well-developed central value, a most likely temperature history. The temperature record has two well-developed minima at AD 1250 and 1850. From 1850 to the present, temperatures have gradually increased by 0.7 K. The reconstructed temperatures are compared with the stable oxygen isotope (δ^{18}O) from the DSS ice core.

TEMPERATURE PROFILE FROM LAW DOME

In 1993 the glaciology group of the Australian Antarctic Division completed the drilling of a 1200 m deep ice core to bedrock 4.68 km south-southwest of the highest point on the Law Dome ice cap (66°46′ S, 112°48′ E; 1370 m a.s.l.) (Morgan and others, 1997). In 1996 a temperature profile was inferred from measurements every 10–20 m in the deep borehole, with a measuring accuracy of 0.02 K (Van Ommen and others, 1999). Temperature measurements in the top 50 m are from the cased part of the deep borehole, above the liquid level, and they are disturbed and influenced by the temperature and pressure conditions in the building constructed over the borehole. They do not represent the undisturbed firn and ice temperatures.

In 1997, temperatures were measured in a 270 m deep dry borehole drilled 80 m south of the deep borehole (Van Ommen and others, 1999). These temperatures have an accuracy of 0.05 K, but are believed to be a better representation of the undisturbed firn and ice temperatures than those from shallow depths in the deep borehole. The two temperature profiles were combined in such a way that the shallow borehole profile was used down to 50 m, the depth zone between 50 and 270 m was used to align the two profiles, and the temperatures from the deep borehole were used below 50 m. The combined temperature profile (Fig. 1a, solid curve) is used to reconstruct the past temperature history. A study of the noise in the data (Fig. 1b) clearly shows the increased errors in the measurements from the shallow borehole. Below 750 m depth, convection cells in the borehole liquid are seen to appear. Temperature excursions in the profile due to these cells increase as the temperature gradient increases (Gundestrup, 1989; Gundestrup and others, 1994; Gundestrup and Clow, 1997). The convection cells are smoothed out before the reconstruction of the past temperatures is attempted, as they do not represent ice temperatures.

A temperature profile assuming steady-state conditions and the present-day ice-sheet configuration (accumulation rate 0.678 m ice a^{-1}; surface temperature −21.2°C; geothermal heat flux 75.1 mW m^{-3}) is calculated and shown as the dashed curve in Figure 1a. Comparison between the measured and the modelled temperatures of Figure 1a provides a first-order estimate on the amount of climate information preserved in the borehole. It is clear that in the past there was a period with colder temperatures, with a recent warming to the present surface conditions. Below 650 m depth the measured temperatures are warmer than the modelled, indicating that there was an even earlier period with warmer temperatures than the present. There is no indication of old colder periods, so we do not expect to find any information on climate conditions during glacial periods in the data.

HEAT AND ICE-FLOW MODEL

In order to calculate how the temperatures through the ice have changed back in time, we need to formulate a coupled heat- and ice-flow equation with boundary conditions. The applied heat-flow equation is (Dahl-Jensen and Johnsen, 1986; Johnsen and others, 1995; Dahl-Jensen and others, 1998):

$$\rho c \frac{\partial T}{\partial t} = \nabla(K \nabla T) - \rho c v \cdot \nabla T + f, \qquad (1)$$

where $T(x, z, t)$ is temperature, t is time, z is distance above bedrock, x is horizontal distance along the flowline, $\rho(z)$ is ice density, $K(T, \rho)$ is the thermal conductivity, $c(T)$ is the specific heat capacity and $f(x, z, t)$ is the heat-production term. The ice velocities, $v(x, z, t)$ control the advective term in the heat-flow model. The heat-flow Equation (1) can be reduced to

https://doi.org/10.3189/172756499781821102 Published online by Cambridge University Press

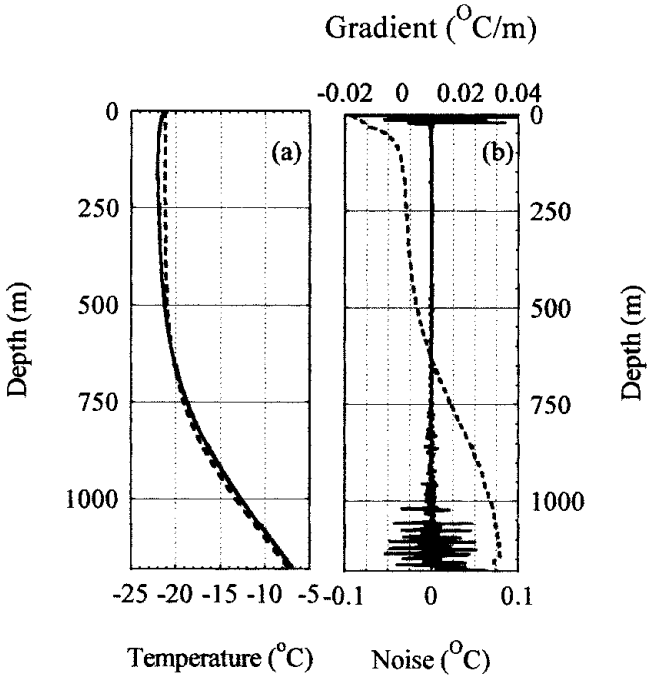

Fig. 1. (a) The measured temperature profile (solid curve) from the Dome Summit South (DSS) borehole on Law Dome, East Antarctica. The top 50 m of the profile is taken from a shallow, air-filled borehole 700 m south of the deep DSS hole. The measured profile is compared to a calculated steady-state profile (dashed curve), assuming present surface conditions. Comparison of the curves shows that there is a recent warming from a colder period seen as colder observed temperatures at 10–700 m depth. From 700 to 1196 m, warmer temperatures are observed, suggesting that there was an earlier warmer period. (b) The noise of the measured temperature profile from (a) (solid curve) is found by comparing the measured data with a smoothed profile. The top 50 m, taken from an air-filled borehole, has deviations up to 0.05 K. Below 700 m depth, the noise is seen to increase with depth. A detailed study of this "noise" shows that it comprises differences formed by convection in the borehole liquid. The amplitude of the disturbances increases with increasing temperature gradient (dashed curve).

a one-dimensional equation in the Law Dome case because the borehole is located close to the summit of the dome where the horizontal velocity, the horizontal derivatives of T and the internal heat production, f, can be neglected:

$$\rho c \frac{\partial T}{\partial t} = \frac{\partial K}{\partial z}\frac{\partial T}{\partial z} + K\frac{\partial^2 T}{\partial z^2} - \rho c v \frac{\partial T}{\partial z}. \qquad (2)$$

The vertical velocity, $w(z,t)$ is approximated by a simple Dansgaard–Johnsen profile (Dansgaard and Johnsen, 1969; Johnsen and Dansgaard, 1992; Morgan and others, 1997) in which the vertical strain rate is constant down to a specified depth (the break depth) and then decreases linearly to zero at the bedrock.

$$w(z,t) = \begin{cases} -a(t)\dfrac{(z-h/2)}{(H-h/2)} & z \in [h, H] \\ -a(t)\dfrac{z^2}{2h(H-h/2)} & z \in [0, h], \end{cases} \qquad (3)$$

where $a(t)$ is the time-dependent accumulation rate, H is the ice-equivalent ice thickness (1178 m) and h is the distance above bedrock of the break point of the vertical strain rate (248 m). H and h are assumed to be constant with time, and $a(t)$ is assumed to vary as a function of the surface temperature $T_{\mathrm{sur}}(t)$:

$$a(t) = a_0 \exp\{\alpha[T_{\mathrm{sur}}(t) - T_0]\}, \qquad (4)$$

where a_0 is the present-day accumulation rate (0.678 m ice a^{-1}) and T_0 is the present-day surface temperature (−21.2°C). α ($\alpha \sim \partial(a/a_0)/\partial T_{\mathrm{sur}}$), the relative change of accumulation rate per °C, determines the temperature effect on the accumulation rate. Estimates of α range from 3–4% from general circulation models to 10% from polar models. Here a value of 7% ($\alpha = 0.07$) has been used with control runs for $\alpha = 0.03$ and 0.10. The equation is based on results from Law Dome (Morgan and others, 1991; Van Ommen and Morgan, 1996), from Vostok (Salamatin and others, 1998) and from similar equations used to describe the accumulation–temperature coupling in Greenland (Dahl-Jensen and others, 1993; Johnsen and others, 1995; Cuffey and Clow, 1997). Recent observations of accumulation changes during the last 30 years have α values as high as 0.5 (Morgan and others, 1991; Peel, 1992), but this is not believed to represent the longer time period treated here. It will be shown later that the reconstructed temperature history spans only the last 4 ka, where surface temperatures have changed by only a few °C, and that there is no memory left of the Last Glacial Maximum. The control runs with $\alpha = 0.03$ and 0.10 vary the reconstructed temperatures by < 0.1 K, so we conclude that the value of α in Equation (4) is not a sensitive parameter for our analysis.

The calculations are started 100 ka back in time, which is far beyond the memory of the system. The applied boundary conditions are:

$$T(z, -100\mathrm{ka}) = T_{\mathrm{ss}}$$
$$(T_{\mathrm{sur}} = -35^\circ\mathrm{C}; a(-35^\circ\mathrm{C});\ Q_{\mathrm{geo}} = 75.1\,\mathrm{mW\,m^{-2}}) \qquad (5a)$$
$$T(H,t) = T_{\mathrm{sur}}(t) \qquad (5b)$$
$$\frac{\partial T}{\partial z}(-3000\,\mathrm{m}, t) = -\frac{Q_{\mathrm{geo}}}{K_{\mathrm{rock}}} \qquad (5c)$$
$$K_{\mathrm{ice}}\frac{\partial T}{\partial z}|_{\mathrm{ice}}\,(0\,\mathrm{m}, t) = K_{\mathrm{rock}}\frac{\partial T}{\partial z}|_{\mathrm{rock}}(0\,\mathrm{m}, t). \qquad (5d)$$

Symbols above are as previously defined, with the addition that Q_{geo} is the geothermal heat flux. A value of 75.1 mW m^{-2} is found (later) to be most probable (see Fig. 2e) for Q_{geo}. The initial boundary condition T_{ss}, (Equation (5a)), is a steady-state temperature profile for glacial conditions. The calculations are started so far back in time that the initial temperature profile will not influence the temperature history through the last 4 ka. The second condition (Equation (5b)) is the unknown temperature history to be reconstructed. The third condition (Equation (5c)) is placed 3 km below the ice/bedrock interface, where all past temperature changes are assumed to be diffused out. The fourth condition (Equation (5d)) assures that the heat is transferred through the ice–rock boundary at the bedrock ($z = 0$), assuming that the ice here has always been below the pressure-melting point. Equations (2)–(5) define the boundary value problem, which can be solved when the temperature history and the geothermal heat flux are known.

The problem is solved with a Crank–Nicholson finite-difference scheme where the depth is divided into steps of 20 m and the maximum time-step is 75 years. The unknown temperature history is assumed to be a smooth curve through 50 values that are to be determined. Temperature

https://doi.org/10.3189/172756499781821102 Published online by Cambridge University Press

values are changed at intervals which vary logarithmically from 12 ka when calculations are commenced ($t = -100$ ka) to 8 a at the present ($t = 0$ a). The calculations in the Crank–Nicholson scheme use time-steps no larger than 20% of the time-varying intervals.

THE MONTE CARLO INVERSE METHOD

A Monte Carlo method has been developed to describe the information on past climate that can be derived from the measured temperature profile (Mosegaard and Tarantola, 1995; Dahl-Jensen and others, 1998; Mosegaard, 1998). The Monte Carlo method tests randomly selected combinations of climate history and geothermal heat flux by using them as input to the coupled heat- and ice-flow model, and considering the resulting degrees of fit between the reproduced and measured temperature profiles.

The Monte Carlo scheme uses a random walk in the high dimensional space of all possible models, m (temperature histories and geothermal heat fluxes). The temperature history has been divided into 50 intervals as described above, so including the geothermal heat flux as an unknown gives a 51-dimensional model. In each step of the random walk a perturbed model, $m^i{}_{\mathrm{pert}}$ of the current model vector m^i is proposed. The next model becomes equal to $m^i{}_{\mathrm{pert}}$ with an acceptance probability $P_{\mathrm{accept}} = \min(1, \exp\{-[S(m^i{}_{\mathrm{pert}}) - S(m^i)]\})$ where $S(m) = \Sigma_j[g^j(m) - d^j{}_{\mathrm{obs}}]^2$ which is the misfit function measuring the difference between $g(m)$, the calculated borehole temperatures, and d_{obs}, the observed temperatures. If the perturbed model is rejected, the next model becomes equal to m^i and a new perturbed model is proposed.

To ensure an efficient sampling of all possible models, different techniques have been developed for choosing the temperature histories and geothermal heat fluxes to be tested. The main scheme to perturb the models is to randomly select one of the 51 temperature/heat-flux parameters and change its value to a new value chosen uniformly at random within a given interval. A singular value decomposition (SVD) of the matrix $G = \{\partial g_j/\partial m_i\}$, evaluated in a near-optimal model, yields a set of eigenvectors in the model space whose orientations reveal efficient directions of perturbation for the random walk. The SVD method is included as a possible method of perturbing models, especially at the start of the process, as it speeds the Monte Carlo scheme significantly.

The results presented here are based on tests of 8×10^6 models. Of the approximately 30% that were accepted by the Monte Carlo scheme, every 500th is chosen where the misfit function S is less than the variance of the observations. Thus, 5500 independent solutions were selected. The step of 500 was chosen to exceed the maximum correlation length of the output model parameters, a necessary condition for the 5500 models to be uncorrelated. To further ensure that the output models were uncorrelated, the random walk was frequently restarted at randomly selected points in the model space. The 5500 climate histories and heat fluxes are sampled with a frequency proportional to their likelihood (Mosegaard and Tarantola, 1995) and all accepted solutions fit the observations within their limits of uncertainty. A statistical analysis leads to the desired estimate of the past climate changes.

RESULTS

Histograms can be made of the sampled geothermal heat

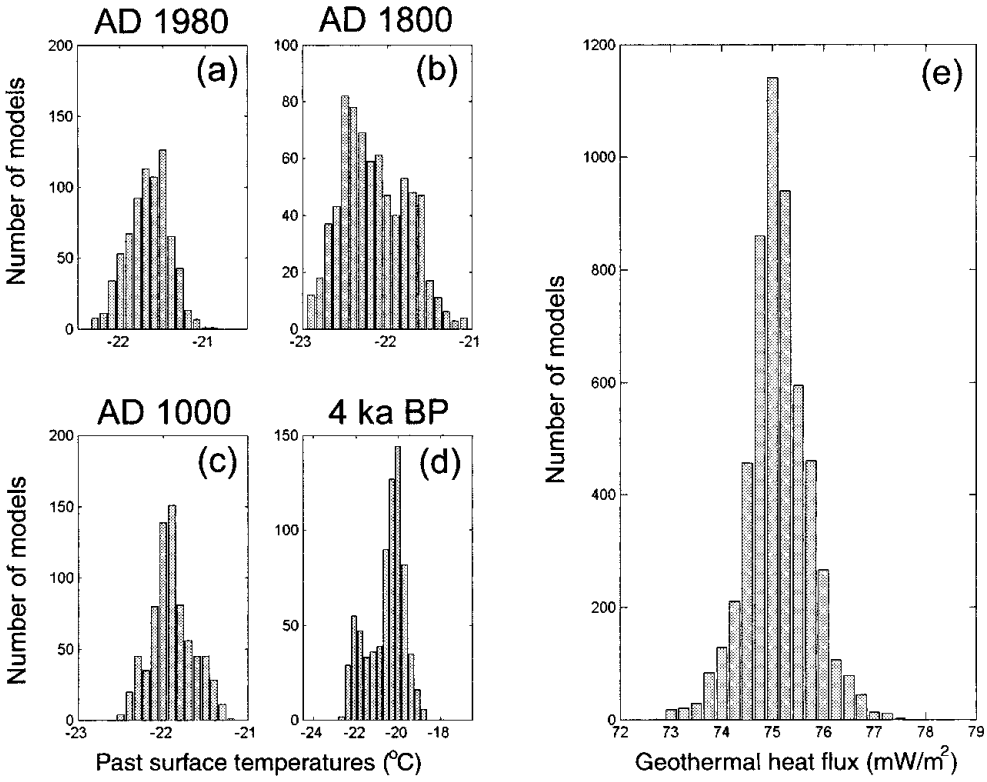

Fig. 2. (a–d) The probability distribution of the past surface temperatures at selected times before present. They are constructed as histograms of the 5500 Monte Carlo sampled and accepted temperature histories. All temperature distributions are seen to have a maximum, a most likely value, which is assumed to be the reconstructed surface temperature at these times. (e) The probability distribution of the accepted geothermal heat fluxes. The most likely value is 75.1 mW m^{-2}.

https://doi.org/10.3189/172756499781821102 Published online by Cambridge University Press

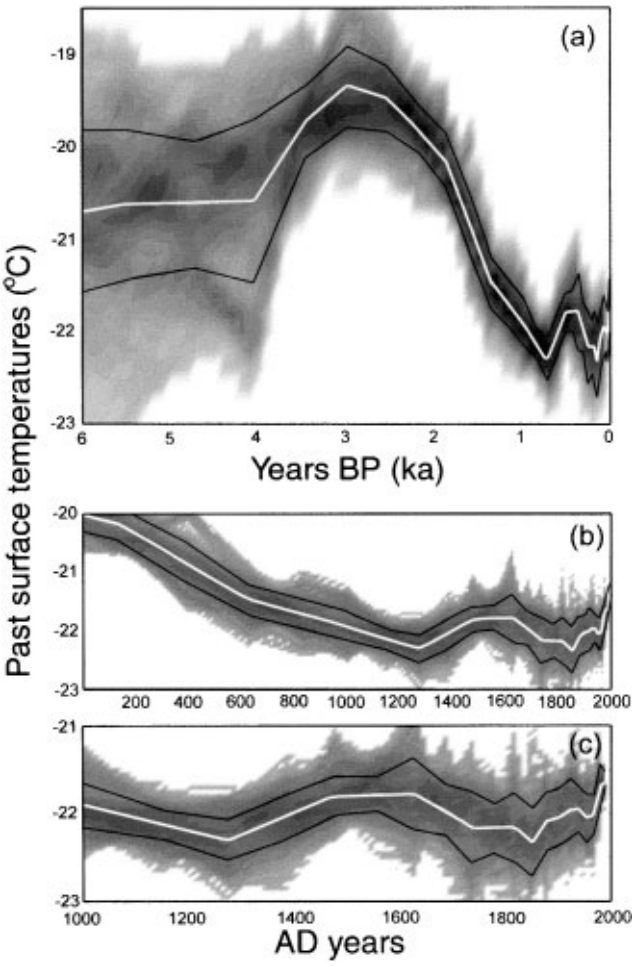

Fig. 3. The contour plots of all the DSS temperature histograms as a function of time describe the reconstructed temperature history (white curve) and its uncertainty. The black curves indicate a measure for the standard deviations of the reconstruction. (a) The last 6 ka. A period 2–4 ka BP has temperatures 2 K warmer than the present. (b) The last 2 ka. A cold period is seen between AD 1300 and 1850. (c) The last 1 ka. The cold period is seen to have minima at AD 1250 and 1790–1850. The temperature has been increasing since AD 1850 and there has been a temperature increase of 0.025 K a^{-1} over the last 30 years.

fluxes and of the temperature histories at given times before present. The probabilistic formulation of the inverse problem leads to the definition of a probability distribution in the model space, describing the likelihood of possible temperature histories and geothermal heat-flow densities. The Monte Carlo scheme is constructed to sample according to this probability distribution. The histograms in Figure 2 describe the probability distribution of the geothermal heat flux and temperatures at selected times before present. The maxima in the histograms thus describe the most likely values. The method does not constrain the distributions to have a single maximum; indeed there could be histograms with several maxima (e.g. Fig. 2b), reflecting the fact that more than one value of the temperature at this time would give a good fit to the observed temperature in the borehole. The histograms however, all have a well-defined zone of most likely past temperatures. A smooth curve is fitted to the histograms, and the maximum value is taken as the most likely value.

Contour plots of the probability distributions of the past surface temperatures are shown in Figure 3. The most likely past temperature history is shown as white curves that represent the maximum values of the distributions such as those shown in Figure 2. The black curves indicate the standard deviations of the probability distributions; they are a measure for how well the past temperatures can be determined. Figure 3a shows the reconstruction of the past surface temperatures for the last 6 ka. The standard deviation increases from 0.1 K at present to >1 K at 4 ka BP.

A forward analysis with the coupled heat- and ice-flow Equations (2)–(5) gives us information on how Gaussian perturbations of the temperature history can be detected in the borehole-temperature profile. The perturbations of the temperature history during the last 4 ka are seen to give well-defined perturbations ("bumps") in the borehole temperatures. The depth of the maximum perturbation in the borehole profile is a function of the location of the perturbation in the time domain. The further back in time the perturbations are placed, the deeper are the maxima found in the borehole. The perturbations in the borehole temperatures are also broadened by diffusion. The deeper and older they are, the more they are diffused out. A perturbation placed further back in time than 4.5 ka no longer has a well-defined maximum in the ice; the maximum has passed down to the underlying rock. The probability distributions of Figure 3a are also seen to broaden for ages older than 4 ka. This reflects the reduced ability to resolve the past temperatures at these ages, so the memory time of the problem is confined to 4 ka.

As described above, the resolution decreases back in time. To maximise computer efficiency without sacrificing resolution, time intervals have been chosen which increase back in time. The time intervals have been selected so that standard deviations of the reconstructed past temperatures are all around 0.3 K for the last 4 ka.

DISCUSSION AND CONCLUSION

The probability distribution of accepted geothermal heat fluxes (Fig. 2e) has a median of 75.1 ± 0.6 mW m^{-2}, a high value for the heat-flow density for the continental crust of Antarctica (Sclater and others, 1980). The memory of temperatures in the ice is only 4 ka, so there are no remnants of the cold glacial temperatures near the bedrock. The reconstructed value for the heat flux is thus given mainly by the basal temperature gradient and can be considered very reliable.

The reconstructed temperature history for the last 4 ka shows a warm period 2–4 ka BP (Fig. 3a). After 2 ka BP, temperatures decrease to a minimum around AD 1300 (Fig. 3b and c). The cold period AD 1300–1850 contains a slight warming around AD 1400–1600, and the coldest period is found at the end (AD 1790–1850). Temperatures have increased since AD 1850, and the mean temperature gradient over the last 30 years is 0.025 K a^{-1}.

Since the reconstructed temperature history is determined from directly observed temperatures in the ice (i.e. remnants of past temperature changes) and not from proxy data such as $\delta^{18}O$, there is no ambiguity associated with calibration of the observed data and the past temperatures (Johnsen and others, 1995; Cuffey and Clow, 1997). The resolution, however, is time-dependent, so temperature events of short duration are detectable if they are very recent, but diffused out if they are older.

The reconstructed temperature history can be compared with other records of past climate over East Antarctica. The

https://doi.org/10.3189/172756499781821102 Published online by Cambridge University Press

most recent history, the last 50 years, can be compared with direct observations (Jones and Wigley, 1988; Jacka, 1990; Jones, 1990; Morgan and others, 1991). The observed warming over the last 30 years (Jacka, 1990) is seen in the reconstructed temperature history as a 0.75 K rise. This is in agreement with an Antarctic average temperature increase of 0.5 K over these 30 years (Jacka, 1990; Peel, 1992; King and Turner, 1997) . The data from Casey station, close to the drill site, support the 0.75 K increase in the Law Dome region (Van Ommen and others, 1999).

For periods reaching back before direct observations are available, the temperature history can be compared with other proxy records of past climate from East Antarctica. The stable-oxygen-isotope record from the Law Dome DSS ice core, i.e. the borehole used in this analysis, is an obvious choice (Morgan, 1985; Morgan and others, 1997). Figure 4 compares the stable isotopes (δ^{18}O) measured in the DSS ice core with the reconstructed temperatures. A general agreement is observed over the last 1 ka. The correlation between the isotopes and temperatures for the last 1 ka has the gradient $\partial(\delta^{18}\mathrm{O})/\partial(T_{\mathrm{sur}}) = 0.6$ [‰/K]. This value is in agreement with that found for near-surface studies in the region (Peel, 1992; Van Ommen and Morgan, 1996; Van Ommen and others, 1999).

Over the last 4 ka an interesting source of information is the presence and abundance of penguins on rookeries along the Victoria Land coast (Baroni and Orombelli, 1994). For the period 4.3–2.8 ka BP, ten sites with penguin colonies have been found in southern Victoria Land compared to only three at present. This "penguin optimum" is believed to correspond with a warm period in agreement with the reconstructed temperature history from the Law Dome borehole. The period with increased surface temperatures at 2–4 ka BP is not seen to the same extent in the stable-oxygen-isotope curve. Two factors that could help to explain the differences are the decrease of ice thickness and the isostatic uplift of the region during and after the deglaciation (Goodwin, 1993).

A 50–200 m greater ice thickness during the glacial at the summit of Law Dome (Goodwin, 1993) would have left warmer basal temperatures and thus would cause us to reconstruct an erroneously warm period 2–4 ka BP due to our assumption of constant ice thickness. The decrease of ice thickness, however, is assumed to have been finalised 6–8 ka BP (Goodwin, 1993), so the maximum decrease of the reconstructed temperature history 4 ka back in time is calculated to be 0.5 K. The isostatic uplift of the Law Dome area has been estimated at 0.5–0.6 m (100 a)$^{-1}$ with a total estimated uplift of 53 m (Goodwin, 1993). This uplift would affect past surface temperatures, and the reconstructed temperature history would thus overestimate the surface temperatures by 0.2 K at 4 ka BP. If the geometry of the Law Dome ice cap was different in the past, the shape of the vertical velocity profile at the drill site may have changed. This would change the amount of cold ice advected through the ice cap and thereby the reconstructed temperature history. If the site was closer to the summit, surface temperatures 2–4 ka BP are overestimated by up to 1 K. If the site was further from the divide, surface temperatures 2–4 ka BP are underestimated by up to 0.5 K.

It is concluded that the reconstructed temperatures could be overestimated by up to 0.7 K for the warm period 2–4 ka BP. This would lead to a reconstructed temperature profile closer to that inferred by the δ^{18}O of the DSS core (Fig. 4). The isotope values recorded in the ice core are also influenced by ice-thickness changes, isostatic uplift and changing atmospheric circulation patterns. Assuming the ice-thickness change had been finalised by 4 ka BP, the surface-elevation changes during the last 4 ka are due to isostatic uplift of the region. This could only account for a 0.1‰ elevation correction of the stable oxygen isotope at 4 ka BP.

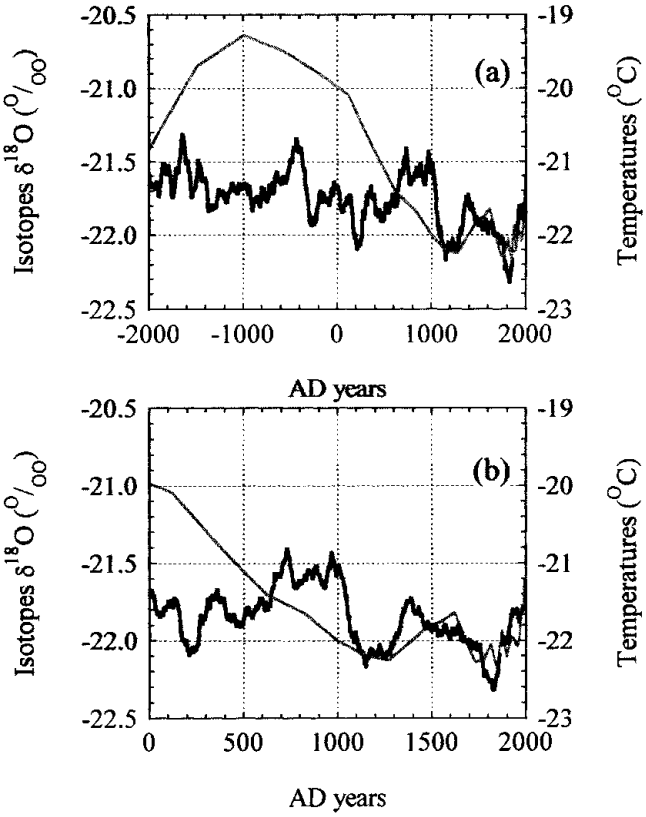

Fig. 4. The stable oxygen isotope ($\delta^{18}O$) is compared to the reconstructed temperature history, both from the DSS site. There is reasonable agreement for the last 1 ka, but the maximum found in the temperature history at 2–4 ka BP is not strongly reflected in the $\delta^{18}O$ values. (a) shows the records for the last 4 ka, while (b) enlarges the most recent 2 ka.

ACKNOWLEDGEMENTS

Part of this work was carried out while D. Dahl-Jensen visited the Antarctic CRC in 1996. D. Dahl-Jensen is grateful for the hospitality received as well as for many fruitful discussions.

REFERENCES

Baroni, C. and G. Orombelli. 1994. Abandoned penguin rookeries as Holocene paleoclimatic indicators in Antarctica. *Geology*, **22**(1), 23–26.

Cuffey, K. M. and G. Clow. 1997. Temperature, accumulation, and ice sheet elevation in central Greenland through the last deglacial transition. *J. Geophys. Res.*, **102**(C12), 26,383–26,396.

Dahl-Jensen, D. and S. J. Johnsen. 1986. Palaeotemperatures still exist in the Greenland ice sheet. *Nature*, **320**(6059), 250–252.

Dahl-Jensen, D., S. J. Johnsen, C. U. Hammer, H. B. Clausen and J. Jouzel. 1993. Past accumulation rates derived from observed annual layers in the GRIP ice core from Summit, central Greenland. *In* Peltier, W. R., *ed. Ice in the climate system*. Berlin, etc., Springer-Verlag, 517–532. (NATO ASI Series I: Global Environmental Change 12.)

Dahl-Jensen, D. *and 6 others*. 1998. Past temperatures directly from the Greenland ice sheet. *Science*, **282**(5387), 268–271.

Dansgaard, W. and S. J. Johnsen. 1969. A flow model and a time scale for the ice core from Camp Century, Greenland. *J. Glaciol.*, **8**(53), 215–223.

Goodwin, I. D. 1993. Holocene deglaciation, sea-level change and the emer-

https://doi.org/10.3189/172756499781821102 Published online by Cambridge University Press

gence of the Windmill Islands, Budd Coast, Antarctica. *Quat. Res.*, **40**(1), 70–80.

Gundestrup, N. S. 1989. Hole liquids. *In* Rado, C. and D. Beaudoing, *eds. Ice core drilling. Proceedings of the Third International Workshop on Ice Drilling Technology, Grenoble — France, 10–14 October 1988.* Grenoble, Centre National de la Recherche Scientifique. Laboratoire de Glaciologie et Géophysique de l'Environnement, 51–53.

Gundestrup, N. S. and G. D. Clow. 1997. Logging of the GRIP and GISP2 boreholes. [Abstract.] *EOS*, **78**(46), Fall Meeting Supplement, F7.

Gundestrup, N. S., H. B. Clausen, S. B. Hansen and S. J. Johnsen. 1994. Hole liquids and gaskets for the Istuk deep ice core drill. *Natl. Inst. Polar Res. Mem., Special Issue* 49, 327–334.

Jacka, T. H. 1990. Antarctic and Southern Ocean sea-ice and climate trends. *Ann. Glaciol.*, **14**, 127–130.

Johnsen, S. J. and W. Dansgaard. 1992. On flow model dating of stable isotope records from Greenland ice cores. *In* Bard, E. and W. S. Broecker, *eds. The last deglaciation: absolute and radiocarbon chronologies*. Berlin, etc., Springer-Verlag, 13–24. (NATO ASI Series I: Global Environmental Change 2.)

Johnsen, S. J., D. Dahl-Jensen, W. Dansgaard and N. S. Gundestrup. 1995. Greenland paleotemperatures derived from GRIP borehole temperature and ice core isotope profiles. *Tellus*, **47B**(5), 624–629.

Jones, P. D. 1990. Antarctic temperatures over the present century — a study of the early expedition record. *J. Climate*, **3**(11), 1193–1203.

Jones, P. D. and T. M. L. Wigley. 1988. Antarctic gridded sea level pressure data: an analysis and reconstruction back to 1957. *J. Climate*, **1**(12), 1199–1220.

King, J. C. and J. Turner. 1997. *Antarctic meteorology and climatology.* Cambridge, Cambridge University Press.

Morgan, V. I. 1985. An oxygen isotope–climate record from the Law Dome, Antarctica. *Climatic Change*, **7**(4), 415–426.

Morgan, V. I., I. D. Goodwin, D. M. Etheridge and C. W. Wookey. 1991. Evidence from Antarctic ice cores for recent increases in snow accumulation. *Nature*, **354**(6348), 58–60.

Morgan, V. I., C. W. Wookey, Li Jun, T. D. van Ommen, W. Skinner and M. F. Fitzpatrick. 1997. Site information and initial results from deep ice drilling on Law Dome, Antarctica. *J. Glaciol.*, **43**(143), 3–10.

Mosegaard, K. 1998. Resolution analysis of general inverse problems through inverse Monte Carlo sampling. *Inverse Problems*, **14**, 405–426.

Mosegaard, K. and A. Tarantola. 1995. Monte Carlo sampling of solutions to inverse problems. *J. Geophys. Res.*, **100**, 12,431–12,447.

Peel, D. A. 1992. Ice core evidence from the Antarctic Peninsula region. *In* Bradley, R. S. and P. D. Jones, *eds. Climate since A.D. 1500.* London and New York, Routledge, 549–571.

Salamatin, A. N., V. Ya. Lipenkov, N. I. Barkov, J. Jouzel, J.-R. Petit and D. Raynaud. 1998. Ice core age dating and paleothermometer calibration based on isotope and temperature profiles from deep boreholes at Vostok Station (East Antarctica). *J. Geophys. Res.*, **103**(D8), 8963–8978.

Sclater, J. G., C. Jaupart and D. Galson. 1980. The heat flow through oceanic and continental crust and the heat loss of the Earth. *Rev. Geophys. Space Phys.*, **18**(1), 289–311.

Van Ommen, T. D. and V. Morgan. 1996. Peroxide concentrations in the Dome Summit South ice core, Law Dome, Antarctica. *J. Geophys. Res.*, **101**(D10), 15,147–15,152.

Van Ommen, T. D., V. I. Morgan, T. H. Jacka, S. Woon and A. Elcheikh. 1999. Near-surface temperatures in the Dome Summit South (Law Dome, East Antarctica) borehole. *Ann. Glaciol.*, **29** (see paper in this volume).

https://doi.org/10.3189/172756499781821102 Published online by Cambridge University Press